INTERNATIONAL JOURNAL FOR NUMERICAL AND ANALYTICAL METHODS IN GEOMECHANICS, VOL. 21, 241–253 (1997)

ANALYSIS OF ROCKBOLT REINFORCEMENT USING BEAM-COLUMN THEORY

SAMIT ROY* AND ANAND B. RAJAGOPALAN**

Rock Mechanics, University of Missouri-Rolla, 114, Rock Mechanics, 1006 Kingshighway, Rolla, MO 65401, U.S.A.
Department of Mechanical Engineering, University of Missouri-Rolla, Rolla, MO 65401, USA

SUMMARY

A simple analytical procedure that applies classical beam-column theory for evaluating passive rockbolt roof reinforcement is presented in this paper. The analytical model is derived from first principles and is capable of modelling any number of reinforcing bolts. Each rockbolt is modelled as a linear spring and the model allows for non-uniform bolt spacing. In this study the rock beam is assumed to be isotropic and linearly elastic for the sake of simplicity. However, the analytical model can be extended to include anisotropic rockmass as well as inelastic material behaviour. The solution to the coupled set of governing equations is obtained by using a simple numerical solution procedure. The results from the analytical model indicate that the critical buckling load of a rock beam is strongly influenced by the ambient rock modulus. For salt-rock excavations the rock modulus typically declines with time due to various phenomena, and a diminished modulus could seriously compromise roof stability. The other main conclusion of this study is that rockbolts loose their effectiveness in restraining a roof beam once its critical buckling load is approached. In such a situation, increasing bolt stiffness does not improve its reinforcing action on a roof beam but it enhances the possibility of bolt failure due to anchor pull-out. © 1997 by John Wiley & Sons, Ltd. Int. j. numer. anal. methods geomech., vol. 21, 241–253 (1997)

(No. of Figures: 8 No. of Tables: 1 No. of Refs: 10)

Key words: rockbolt; Euler–Bernoulli; beam-column; roof-reinforcement; stability; pull-out

1. INTRODUCTION

The structural response of rock masses is quite complex because of the existence of joints and discontinuities. Mining related excavations and loading processes applied to rock masses can trigger instability at these discontinuities. The strength and deformational properties of a rock mass can be improved by inserting rockbolts or dowels as stabilizing reinforcements. Numerous types of rockbolts have been developed and applied for this purpose for several decades. In spite of the widespread use of rockbolts and dowels, particularly by the mining industry, the design and application of rock bolts is still largely empirical. However, a growing public awareness for safety and a need to reduce operational cost require a more scientific approach to the design and installation of rock reinforcement.

* Senior Research Investigator and Assistant Professor of Engineering Mechanics
Correspondence to: Samit Roy, Senior Investigator in Rock Mechanics and Assistant Professor of Engineering Mechanics, University of Missouri-Rolla, 114 Rock Mechanics, 1006 Kingshighway, Rolla, MO 65401 USA
** Graduate Research Assistant

CCC 0363–9061/97/040241–13$17.50

Received 15 February 1996
Revised 20 August 1996

It has now been recognized that precise analysis of the mechanisms of rockbolt reinforcement and the behaviour of reinforced rock masses is necessary for the safe design of rock structures. The three main approaches proposed for the analysis of jointed reinforced rock masses are key block analysis,[1] discrete joint analysis,[2] and 'equivalent material' analysis based on principles of continuum mechanics.[3] Researchers have developed sophisticated finite element procedures for both discrete rockbolt/joint model[4–6] and the 'equivalent material' model.[7–9] While the modelling accuracy of the finite element procedure is clearly superior for complex structural geometries and non-linear material behaviour, simple closed-form solutions can effectively be employed for certain design applications as discussed in the following paragraph.

The objective of this paper is to develop a simple design procedure for rockbolt reinforcement in underground excavations using a discrete modelling approach that applies basic principles of engineering mechanics. Specifically, the paper addresses the situation where rock bolts are employed to reinforce the roof of an underground excavation such as shown in Figure 1. While advanced computational techniques such as the finite element method may be used to perform the necessary design calculations discussed here, considerable time and effort must be expended in preparation of input data for the finite element solver and in processing the voluminous output. Also, obtaining appropriate material parameters is frequently not straightforward. The procedure outlined in this paper provides a rockbolt failure prediction methodology

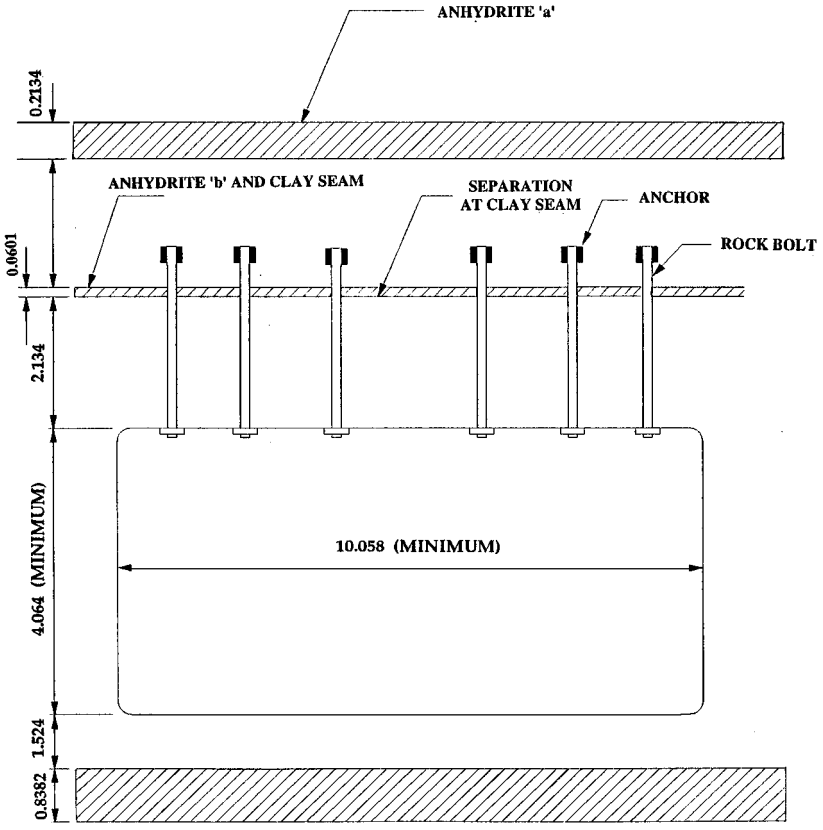

Figure 1. Application of rock bolts to support roof beam (all dimensions in m)

that is very efficient, and it requires very little input preparation that makes it readily useable in the field.

2. ANALYTICAL APPROACH

The reinforcing action of rockbolts in jointed rock in the roof of an excavation is shown schematically in Figure 1. As depicted in the figure, the rockbolts are inserted through the rockmass below the discontinuity into the rockmass above. Although pre-tensioning of the bolts could be included in the formulation, it is assumed for simplicity that the rockbolts provide passive reinforcement. Since the bolts are slender and offer little resistance to bending, they are treated as linear springs subjected to tension. Due to the nature of the roof loading considered in this study, shear stiffness of the bolts is not included in the model. Although anisotropy and inelasticity can be included in the model, in this study the intact rock is considered as isotropic and linearly elastic for simplicity.

The rockmass below the discontinuity is idealized as a Euler–Bernoulli beam-column with built-in ends and with discrete springs simulating the rockbolt reinforcements as shown in Figure 2. The external forces acting on the rockmass modelled as a beam-column are (a) weight of the rockmass and reactions at the supports, (b) axial compression and bending moment due to geostatic forces, and (c) the restoring forces due to the passive rockbolts. Invoking symmetry, only one-half of the rockmass is modelled which is divided into n subregions employing $n-1$ rock bolts. The total number of rock bolts in the model is therefore equal to $2(n-1)$. For analytical convenience, it is assumed that an even number of rockbolts is employed. However, the formulation allows the bolt spacings to be completely arbitrary.

A free-body diagram of the rockmass beam-column is shown in Figure 3. The governing equations used in the model are developed based on the free-body diagram.

The various parameters used in the formulation are defined as follows:

p weight per unit length of beam
a_i spacing between bolt i and bolt $(i-1)$
L the beam length
h the width of beam
b the depth of beam

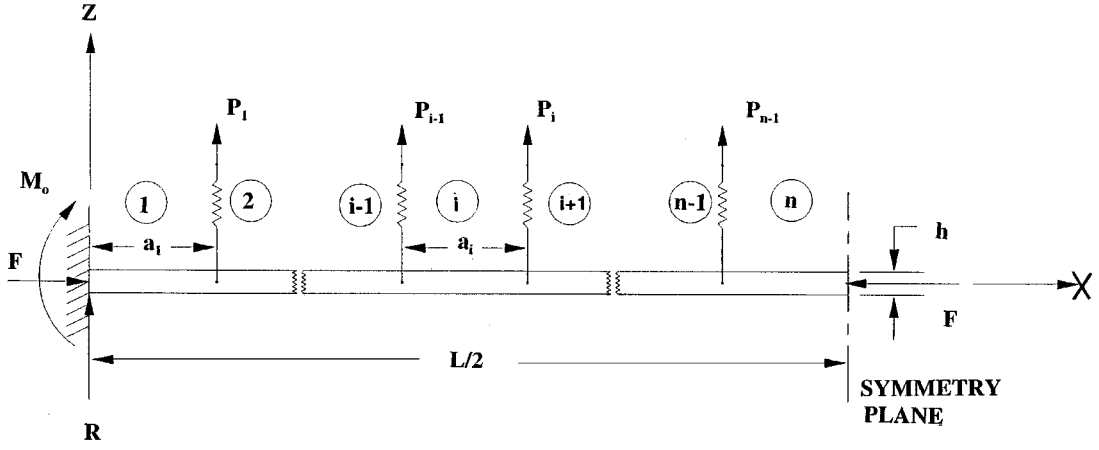

Figure 2. Rock mass idealized as beam column with built-in ends

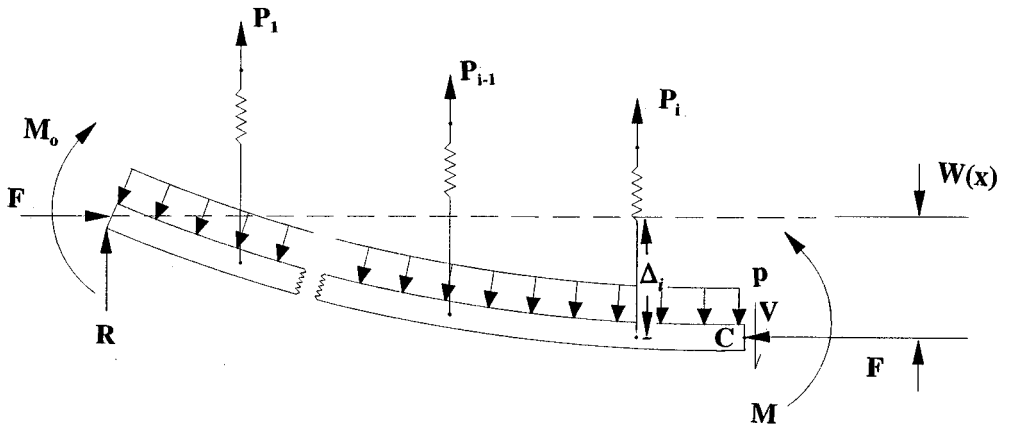

Figure 3. Free-body diagram beam column

w the vertical deflection of the beam at any location x
Δ_i the vertical deflection at ith bolt
M_0 the bending moment at fixed end
K_0 the curvature at the fixed end
F axial compressive force at fixed end
P_i axial force in the ith bolt
k elastic stiffness of rockbolt
E_R modulus of elasticity of rock
I area moment of inertia of beam
E_b modulus of elasticity of bolt
D_b diameter of bolt
L_b effective length of bolt

In subregion n: Considering the moment equilibrium about point C, $\sum M_C = 0$,

$$EI\frac{d^2w}{dx^2} + M_0 + Fw + Rx + P_1(x - a_1) + P_2(x - a_1 - a_2) + \ldots$$

$$+ P_{n-1}(x - a_1 \ldots - a_{n-1}) - \tfrac{1}{2}px^2 = 0$$

Compacting using summation notation,

$$EI\frac{d^2w}{dx^2} + Fw = \frac{1}{2}px^2 - Rx - \sum_{j=1}^{n-1} P_j\left(x - \sum_{r=1}^{j} a_r\right) - M_0 \tag{1}$$

Homogeneous form of equation (1) is given by

$$w'' + \lambda^2 w = 0$$

where

$$\lambda^2 = \frac{F}{EI}$$

and prime denotes differentiation with respect to x.

Hence, the homogeneous solution is

$$w_H = A_n \cos \lambda x + B_n \sin \lambda x$$

Particular solution:

$$w_p'' + \lambda^2 w_p = \frac{\lambda^2}{F}\left[\frac{1}{2}px^2 - Rx - \sum_{j=1}^{n-1} P_j\left(x - \sum_{r=1}^{j} a_r\right) - M_0\right] \tag{2}$$

Let the particular solution be given by

$$w_p = \frac{1}{F}\left[\frac{1}{2}px^2 - Rx - \sum_{j=1}^{n-1} P_j\left(x - \sum_{r=1}^{j} a_r\right) - M_0 + C\right] \tag{3}$$

Substituting (3) in (2),

$$C = \frac{-p}{\lambda^2}$$

General solution for subregion n:

$$W_n = W_H + W_p$$

$$w_n = A_n \cos \lambda x + B_n \sin \lambda x + \frac{1}{F}\left[\frac{1}{2}px^2 - Rx - \sum_{j=1}^{n-1} P_j\left(x - \sum_{r=1}^{j} a_r\right) - M_0 - \frac{p}{\lambda^2}\right] \tag{4}$$

Boundary conditions: From symmetry at mid-span,

$$\left.\frac{\mathrm{d}w}{\mathrm{d}x}\right|_{x=L/2} = 0$$

or

$$w'\left(\frac{L}{2}\right) = -A_n \lambda \sin \lambda \frac{L}{2} + B_n \lambda \cos \lambda \frac{L}{2} + \frac{1}{F}\left[\frac{pL}{2} - R - \sum_{j=1}^{n-1} P_j\right] = 0$$

But from $\sum F_{\text{VERTICAL}} = 0$,

$$R - \frac{pL}{2} + \sum_{j=1}^{n-1} P_j = 0$$

Hence,

$$-A_n \lambda \sin \frac{\lambda L}{2} + B_n \lambda \cos \frac{\lambda L}{2} = 0$$

or

$$B_n = A_n \tan \frac{\lambda L}{2} \tag{5}$$

A similar solution strategy is adopted for the $(n-1)$th subregion.

From moment equilibrium about point C, $\sum M_C = 0$,

$$EI \frac{\mathrm{d}^2 w}{\mathrm{d}x^2} + Fw = \frac{1}{2}px^2 - Rx - \sum_{j=1}^{n-2} P_j\left(x - \sum_{r=1}^{j} a_r\right) - M_0$$

Employing results derived for subregion n, the general solution for subregion $(n-1)$ is

$$w_{n-1} = A_{n-1}\cos\lambda x + B_{n-1}\sin\lambda x + \frac{1}{F}\left[\frac{1}{2}px^2 - Rx - \sum_{j=1}^{n-2} P_j\left(x - \sum_{r=1}^{j} a_r\right) - M_0 - \frac{p}{\lambda^2}\right]$$

From continuity of displacements between the nth and $(n-1)$th subregions,

$$w_{n-1}\left(\sum_{r=1}^{n-1} a_r\right) = w_n\left(\sum_{r=1}^{n-1} a_r\right)$$

or

$$A_{n-1}\cos\lambda\beta_{n-1} + B_{n-1}\sin\lambda\beta_{n-1} = A_n\cos\lambda\beta_{n-1} + B_n\sin\lambda\beta_{n-1} \tag{6}$$

where

$$\beta_{n-1} = \left(\sum_{r=1}^{n-1} a_r\right)$$

Similarly, from continuity of slopes at $x = \beta_{n-1}$,

$$w'_{n-1}[\beta_{n-1}] = w'_n[\beta_{n-1}]$$

$$-A_{n-1}\sin\lambda\beta_{n-1} + B_{n-1}\cos\lambda\beta_{n-1} = -A_n\sin\lambda\beta_{n-1} + B_n\cos\lambda\beta_{n-1} - \frac{P_{n-1}}{F\lambda} \tag{7}$$

Multiplying equation (6) by $\sin\lambda\beta_{n-1}$, and equation (7) by $\cos\lambda\beta_{n-1}$ and adding the results,

$$B_{n-1} = B_n - \frac{P_{n-1}}{F\lambda}\cos\lambda\beta_{n-1} \tag{8}$$

Combining (6) and (8),

$$A_{n-1} = A_n + \frac{P_{n-1}}{F\lambda}\sin\lambda\beta_{n-1} \tag{9}$$

Conversely,

$$\begin{aligned} A_n &= A_{n-1} - \frac{P_{n-1}}{F\lambda}\sin\lambda\beta_{n-1} \\ B_n &= B_{n-1} + \frac{P_{n-1}}{F\lambda}\cos\lambda\beta_{n-1} \end{aligned} \tag{10}$$

Following a similar solution procedure for the ith subregion gives,

$$w_i = A_i\cos\lambda x + B_i\sin\lambda x + \frac{1}{F}\left[\frac{1}{2}px^2 - Rx - \sum_{j=1}^{i-1} P_j\left(x - \sum_{r=1}^{j} a_r\right) - M_0 - \frac{p}{\lambda^2}\right]$$

$$\begin{aligned} A_i &= A_{i-1} - \frac{P_{i-1}}{F\lambda}\sin\lambda\beta_{i-1} \\ B_i &= B_{i-1} + \frac{P_{i-1}}{F\lambda}\cos\lambda\beta_{i-1} \end{aligned} \tag{11}$$

where $2 \leqslant i \leqslant n$.

Note that the equations (11) are valid for $i \neq 1$.

Special case: *subregion* 1. Using previous results, the general solution in subregion 1 is given by

$$w_1(x) = A_1 \cos \lambda x + B_1 \sin \lambda x + \frac{1}{F}\left[\frac{1}{2}px^2 - Rx - M_0 - \frac{p}{\lambda^2}\right]$$

Boundary conditions: Assuming built-in support at $x = 0$,

$$w_1(0) = 0 = A_1 - \frac{1}{F}\left[M_0 + \frac{p}{\lambda^2}\right]$$

or

$$A_1 = \frac{1}{F}\left[M_0 + \frac{p}{\lambda^2}\right] \tag{12}$$

Also, since slope is zero at $x = 0$,

$$w'(0) = 0 = B_1 \lambda - \frac{R}{F}$$

or

$$B_1 = \frac{R}{F\lambda} \tag{13}$$

Using recursive expressions derived in (10),

$$A_n = A_{n-1} - \frac{P_{n-1}}{F\lambda} \sin \lambda\beta_{n-1} = A_{n-2} - \left[\frac{P_{n-2}}{F\lambda} \sin \lambda\beta_{n-2} + \frac{P_{n-1}}{F\lambda} \sin \lambda\beta_{n-1}\right]$$

$$= A_1 - \sum_{j=1}^{n-1}\left[\frac{P_j}{F\lambda} \sin \lambda\beta_j\right]$$

Substituting results from (12), for all $n > 1$,

$$A_n = \frac{M_0}{F} + \frac{p}{F\lambda^2} - \sum_{j=1}^{n-1}\left[\frac{P_j}{F\lambda} \sin \lambda\beta_j\right]$$

$$B_n = \frac{R}{F\lambda} + \sum_{j=1}^{n-1}\left[\frac{P_j}{F\lambda} \cos \lambda\beta_j\right] \tag{14}$$

From (5),

$$B_n = A_n \tan \frac{\lambda L}{2}$$

or

$$\frac{R}{F\lambda} + \sum_{j=1}^{n-1}\left[\frac{P_j}{F\lambda} \cos \lambda\beta_j\right] = \left[\frac{M_0}{F} + \frac{p}{F\lambda^2} - \sum_{j=1}^{n-1}\left(\frac{P_j}{F\lambda} \sin \lambda\beta_j\right)\right] \tan \frac{\lambda L}{2}$$

Substituting in the above equation the force in the jth rockbolt as $P_j = k\Delta_j$, where

$$k = \frac{E_b \prod D_b^2}{4L_b}$$

and the support moment as $M_0 = E_R I K_0$, where

$$I = \frac{1}{12} bh^3$$

gives

$$\frac{1}{\lambda}\sum_{j=1}^{n-1}\left[\frac{1}{\tan\frac{\lambda L}{2}} - \frac{\cos\lambda\beta_j}{\tan\frac{\lambda L}{2}} - \sin\lambda\beta_j\right] k\Delta_j + E_R I K_0 = -\frac{p}{\lambda^2} + \frac{pL}{2\lambda\tan\frac{\lambda L}{2}} \tag{15}$$

The deflection at the location of the $(i-1)$th rockbolt can now be obtained by combining equations (11) and (14), for $2 \leqslant i \leqslant n$ and $i \leqslant j \leqslant n-1$,

$$\Delta_{i-1} = w_i\left(\sum_{r=1}^{i-1} a_r\right)$$

or

$$\Delta_{i-1} = A_i\cos\lambda\beta_{i-1} + B_i\sin\lambda\beta_{i-1} + \frac{1}{F}\left[\frac{1}{2}p\beta_{i-1}^2 - R\beta_{i-1} - \sum_{j=1}^{i-1} P_j(\beta_{i-1} - \beta_j) - M_0 - \frac{p}{\lambda^2}\right]$$

Substituting for A_i and B_i from (11),

$$\begin{aligned}&\sum_{j=1}^{i-1}\left[\frac{1}{\lambda}(\cos\lambda\beta_j - 1)\sin\lambda\beta_{i-1} - \frac{1}{\lambda}\sin\lambda\beta_j\cos\lambda\beta_{i-1} + \beta_j\right]P_j \\ &\quad + \left(\beta_{i-1} - \frac{1}{\lambda}\sin\lambda\beta_{i-1}\right)\sum_{j=i}^{n-1} P_j + (\cos\lambda\beta_{i-1} - 1)M_0 \\ &= F\Delta_{i-1} + \frac{pL}{2}\beta_{i-1} - \frac{pL}{\lambda}\sin\lambda\beta_{i-1} - \frac{p}{\lambda^2}\cos\lambda\beta_{i-1} - \frac{1}{2}p\beta_{i-1}^2 + \frac{p}{\lambda^2}\end{aligned} \tag{16}$$

Substituting $P_j = k\Delta_j$ and $M_0 = E_R I K_0$ in (16),

$$\begin{aligned}&\sum_{j=1}^{i-2}\left[\frac{1}{\lambda}(\cos\lambda\beta_j - 1)\sin\lambda\beta_{i-1} - \frac{1}{\lambda}\sin\lambda\beta_j\cos\lambda\beta_{i-1} + \beta_j\right]k\Delta_j \\ &\quad + \beta_{i-1} - \frac{1}{\lambda}\sin\lambda\beta_{i-1} - F)\,k\Delta_{i-1} + \left(\beta_{i-1} - \frac{1}{\lambda}\sin\lambda\beta_{i-1}\right)k\sum_{j=i}^{n-1}\Delta_j \\ &\quad + (\cos\lambda\beta_{i-1} - 1)E_R I K_0 = p\left[\frac{1}{2}L\beta_{i-1} - \frac{L}{2\lambda}\sin\lambda\beta_{i-1} - \frac{1}{\lambda^2}\cos\lambda\beta_{i-1} - \frac{1}{2}\beta_{i-1}^2 + \frac{1}{\lambda^2}\right]\end{aligned} \tag{17}$$

Equations (15) and (17) provide n equations in the n unknowns $\Delta_1, \Delta_2, \ldots, \Delta_{n-1}$ and K_0. The system of equations can be written in a more compact form by using matrix notation,

$$[A]\{d\} = \{f\} \tag{18}$$

The solution to the coupled linear system of equations can be readily obtained by Gaussian elimination,

$$\{d\} = [A]^{-1}\{f\} \tag{19}$$

Using the equations derived above, a short program (BOLT) was written in FORTRAN 77. The input to the program consists of rock beam dimensions, rock modulus and density, rock bolt dimensions and their locations, and mine depth. Using this input, the program calculates the load in each rockbolt, the deflection of the rock beam at the locations where each rockbolt is attached, and the moment and curvature of the rock beam at the built-in end. Due to its low memory and CPU requirement, the program can readily be run on a generic personal computer.

3. NUMERICAL EXAMPLES

To demonstrate the feasibility of using the proposed analytical model for design evaluation, a practical application of the model for evaluating roof reinforcement in the Waste Isolation Pilot Plant (WIPP) is presented in this section. WIPP is being developed by the U.S. Department of Energy (DOE) as a pilot plant to demonstrate the safe disposal of transuranic waste. The facility, which is located in southeastern New Mexico, is excavated in thick bedded salt at a depth of 655 m (2150 ft). As discussed in Reference 10, the roof support system designed for the waste storage rooms consists of a patterned rock bolting as shown in Figure 4. The rock bolt system consists of mechanically anchored bolts that are approximately 19 mm (3/4 in) in diameter and 3·048 m (120 in) long and are installed according to the pattern shown in Figures 4 and 1. A beam width of 1·18 m (47 in) is selected as shown in Figure 4. The various input parameters used in this analysis are given in Table I. For simplicity, the value of *in situ* stress ratio was assumed to be unity in computing the nominal horizontal compressive force given in Table I.

Figure 5 depicts the effect of horizontal compressive load on rock beam stability for different rock moduli. Rock beam instability manifests itself as a sharp rise in the load carried by the restraining rockbolts. Even though the pull-out load for the rockbolts in this study is approximately 200 kN, the steepness of the maximum load curve at the point of instability implies a low

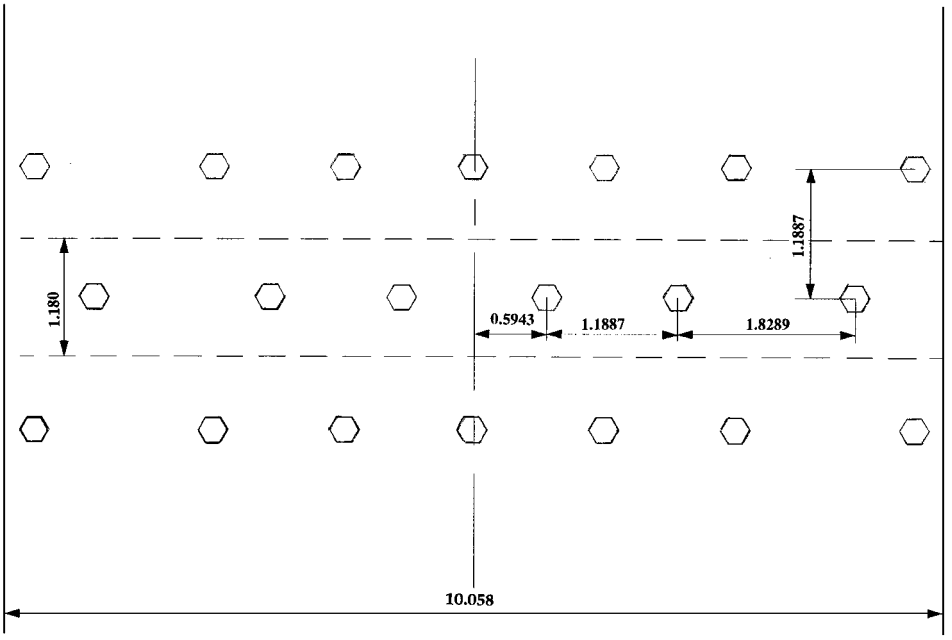

Figure 4. Rock bolt pattern used at WIPP for roof reinforcement (in meters).

Table I. Input parameters

Total number of rockbolts	6
Length of rock segment	10·058 m
Width of rock segment	1·180 m
Height of rock segment	2·134 m
Young's modulus of salt rock	31 GPa
Young's modulus of bolt	207 GPa
Horizontal force acting on the rock segment	37·15 MN
Mass density of salt rock	2300 kg/m^3
Separation distance between adjacent rockbolts (a_1, a_2, a_3)	1·4171 m
	1·8289 m
	1·1887 m
WIPP mine depth	655 m
Diameter of rockbolt	0·01905 m
Length of rockbolt	3·048 m
Elastic stiffness of rockbolt	19·3569 MN/m

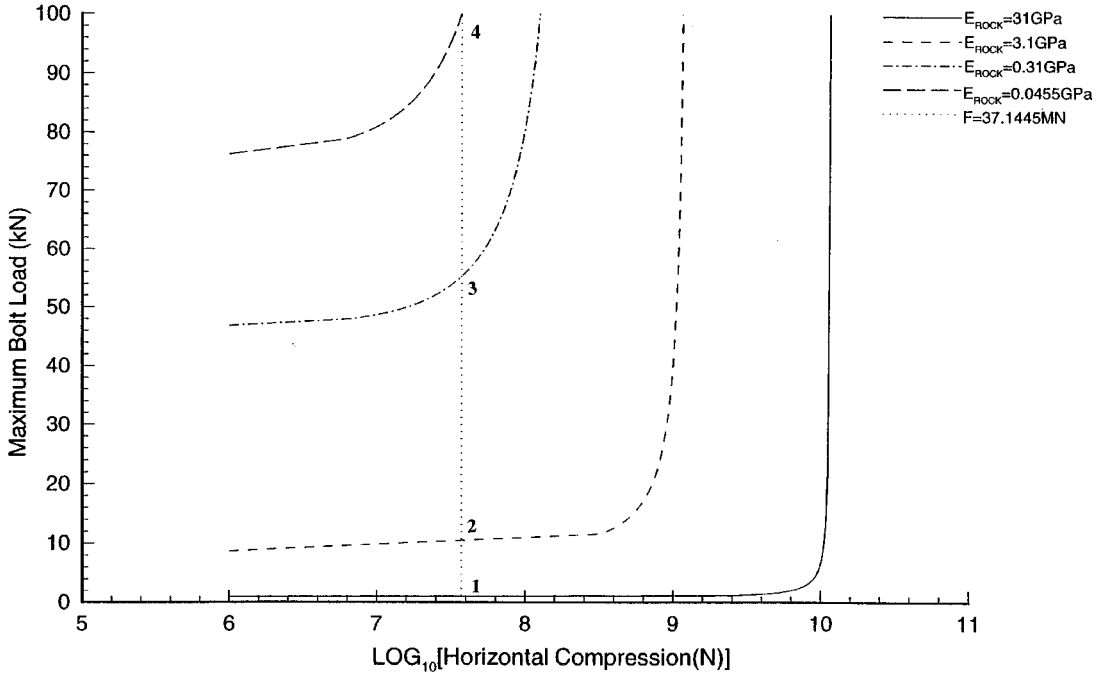

Figure 5. Variation of maximum bolt load with horizontal compression for different rock moduli

margin of safety once the instability load has been approached. It is evident from these curves that rockbolts become less effective in constraining the roof beam deformation as the critical buckling load is approached. Figure 5 also shows the effect of rock modulus on the instability behaviour. A lower rock modulus leads to elevated bolt loads prior to the instability point. However, the nature of the instability becomes progressively benign with decreasing rock modulus as can be observed from the more rounded shape of the parametric curves at the 'knee'. The vertical dotted

line in Figure 5 represents a horizontal compression of 37·15 MN, which is the ambient compressive force at the beam ends due to geostatic stresses at a depth of 655 m. The point of intersection of the vertical dotted line with each of the load curves determines the maximum bolt load for a rock beam with a given modulus. The load curve for intact salt-rock with a modulus of 31 GPa is shown by the solid line in Figure 5. The predicted maximum bolt load for this case is negligibly small, as indicated by its point of intersection with the vertical dotted line and designated as point 1 in the figure. However, in the event the salt-rock beam experiences a reduction in modulus due to a combination of phenomena such as elevated temperature, viscoelastic creep, and evolution of micro-damage due to creep, there could be a dramatic increase in the maximum bolt load as indicated by points 2, 3 and 4 in Figure 5. In fact, as indicated by point 4, extensive reduction in the rock modulus could lead to unstable behaviour even at the ambient compressive load.

Figure 6 depicts the effect of rock modulus on the critical horizontal compressive load for the rock beam with rockbolt reinforcement. The critical horizontal compressive load for a given rock modulus was obtained from the parametric curves shown in Figure 5 by determining the horizontal load at which the bolt load shows a sharp increase in magnitude. The almost linear shape of the log–log plot suggests that for this specific example, the critical buckling load is related to the rock modulus by a power law of the form $F_c = A(E_r)^n$. Figure 7 shows the effect of normalized rockbolt stiffness, K_B, on beam deflection. The normalized rockbolt stiffness is the ratio of the actual bolt stiffness used in each analysis to the nominal bolt stiffness listed in Table I. In Figure 7, the rock beam deflections for various bolt stiffness have been normalized by the mid-span deflection of the rock beam in the absence of rockbolt reinforcement, that is, when $K_B = 0$. The other input parameters used in generating this set of parametric curves are the same as given in Table I. It is noteworthy that a hundredfold increase in bolt stiffness results in only a twofold decrease in beam deflection at the mid-span. On the other hand, a hundredfold increase

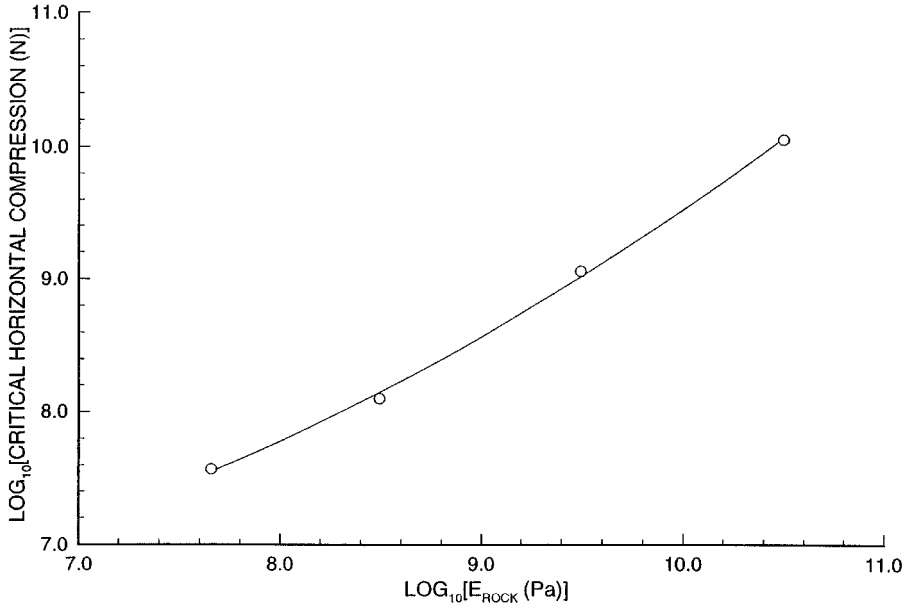

Figure 6. Effect of rock modulus on critical buckling load

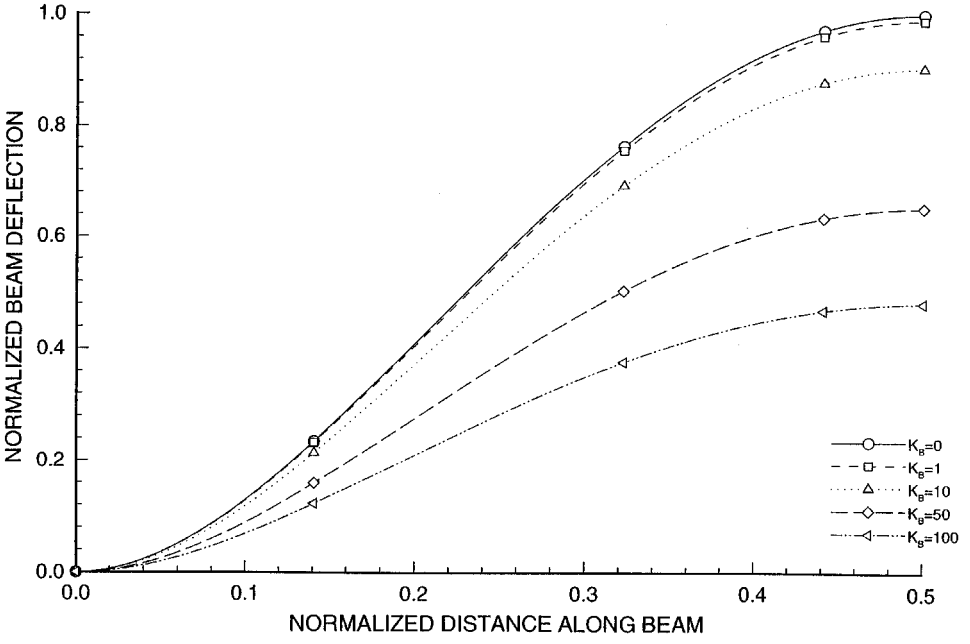

Figure 7. Effect of bolt stiffness on beam deflection

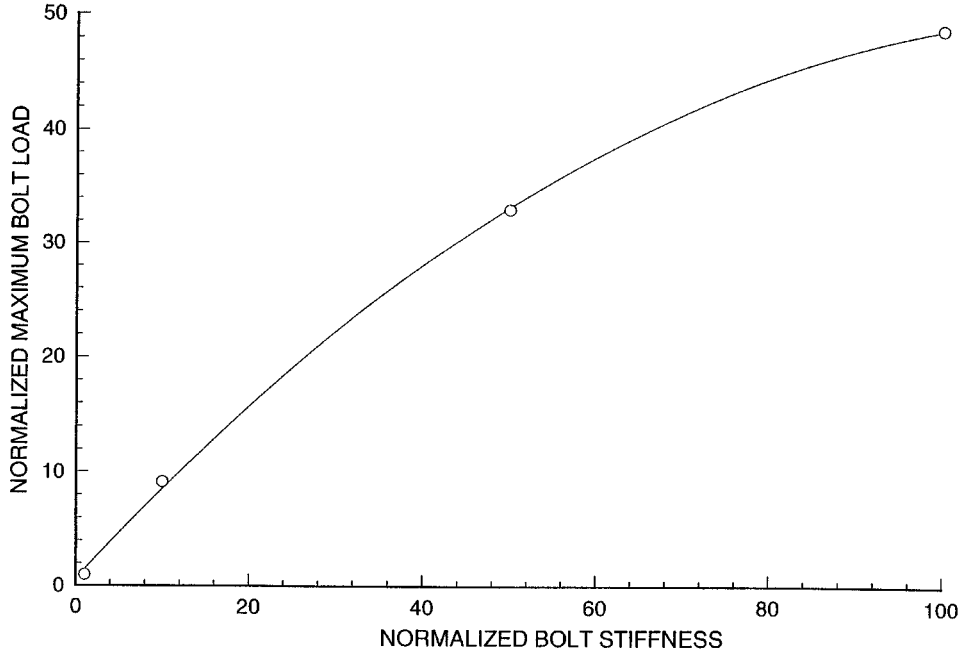

Figure 8. Effect of bolt stiffness on maximum bolt load

in bolt stiffness results in a fiftyfold increase in the total load carried by the bolt nearest to the mid-span as shown in Figure 8. In this figure, the normalized maximum bolt load is the ratio of the maximum load carried by a set of 'stiffer' bolts to the maximum load carried by an identical set of bolts with nominal stiffness. The results in Figure 8 indicate that the use of stiffer bolts for roof beam reinforcement, while providing a stiffer restraint on beam deflection, could significantly increase the chance of failure due to bolt anchor pull-out.

4. CONCLUSIONS

A simple design procedure that applies classical beam-column theory for evaluating passive rockbolt roof reinforcement is presented in this paper. The analytical model is derived from first principles and is capable of modelling any number of reinforcing bolts. Each rockbolt is modelled as a linear spring in tension and the model allows for non-uniform bolt spacings. In this study the rock beam is assumed to be isotropic and linearly elastic for simplicity. However, the analytical model can be extended to include anisotropic rockmass as well as inelastic material behaviour. The solution to the coupled set of governing equations is obtained by using a simple numerical procedure. Roof beam reinforcement used in the WIPP facility is modelled to demonstrate proof-of-concept. The results from the analytical model indicate that the critical buckling load of a rock beam is strongly influenced by the ambient rock modulus. For salt-rock excavations the rock modulus value typically decays with time due to various phenomena, which could ultimately compromise roof stability. The other main conclusion of this study is that rockbolts lose their effectiveness in restraining a roof beam once the critical buckling load is approached. In such a situation, increasing bolt stiffness does not improve its reinforcing action on roof beam but instead it enhances the possibility of bolt failure due to anchor pull-out.

ACKNOWLEDGEMENTS

The authors would like to acknowledge the contribution of Dr. Hamish Miller at the University of Missouri-Rolla, for sharing his expertise in rock reinforcement and for encouraging the authors to develop a practical rockbolt design evaluation procedure. The authors would also like to thank Mr. Srinivas Denduluri for his help in preparing this manuscript.

REFERENCES

1. R. E. Goodman, G.-H. Shi and W. Boyle, 'Calculation of support for hard jointed rock using the key block principle', *Proc. 23rd Symp. on Rock Mechanics*, Berkeley, 1982.
2. T. F. Cho and C. Lee, 'A new discrete rockbolt element for finite element analysis', *Int. J. Rock Mech. Min. Sci. Geomech. Abstr.*, **30,** 1307–1310 (1993).
3. K. G. Sharma and G. N. Pande, 'Stability of rock masses reinforced by passive, fully-grouted rocks bolts', *Int. J. Rock Mech. Min. Sci. Geomech. Abstr.*, **25,** 273–285 (1988).
4. P. A. Cundall, J. Marti, N. Last and M. Asgian, 'Computer modelling of jointed rock masses', *Technical Report N-78-4*, U.S. Army Corps of Engineers, Waterways Experiment Station, Vicksburg, MS, 1978.
5. R. E. Goodman, R. L. Taylor and T. Brekke, 'A model for mechanics of jointed rock', *J. Soil Mach., Found. Div. Am. Soc, Civ. Eng.*, **94**(SM3)**,** 637–659 (1968).
6. C. St John and D. Van Dillen, Rock Bolts, 'A new numerical representation and its application in tunnel design', *Proc. 24th U.S. Symp. on Rock Mechanics*, Texas, 1983, pp. 13–25.
7. O. C. Zienkiewicz and G. N. Pande, 'Time dependent multi-laminate model for rocks—a numerical study of deformation and failure of rock masses', *Int. j. numer. analyt. methods geomech.* 219–247 (1977).
8. C. M. Gerrard, 'Joint compliances as a basis for rock mass properties and the design of supports', *Int. J. Rock Mech. Min. Sci. Geomech. Abstr.*, **19,** 285–305 (1982).
9. C. M. Gerrard and G. N. Pande, 'Numerical model of reinforced jointed rock masses. I', *Theory. Comput. Geotech.* **I**, 293–318 (1985).
10. J. B. Case, C. A. Givens and J. R. Tybursky, 'The geotechnical effects of alcove excavation on panel 1', *Final Report to DOE from IT Corporation, Report No. DOE/WIPP 91-017*, 1991.

